

A Bachelor Thesis by: Micah J.M. van der Vaart.

Supervised by: prof. dr. Andries Meijerink

Influence of the Pr^{3+} concentration in $\text{NaLaF}_4:\text{Pr}^{3+}$ on the radiative decay.

Carried out at the research group:

Condensed Matter and Interfaces

Debye Institute for Nanomaterial Science

Utrecht University



Universiteit Utrecht

January 27th 2014

Abstract

Understanding of luminescence processes and the discovery of novel phosphors is of increasing importance. With the possibility of replacing mercury gas in fluorescent tubes novel phosphors are necessary with increased efficiency. In this thesis the luminescence and quantum cutting of $\text{NaLaF}_4:\text{Pr}^{3+}$ is investigated. $\text{NaLaF}_4:\text{Pr}^{3+}$ samples with varying concentrations of Pr^{3+} were studied. Luminescence decay curves and emission spectra were recorded and analyzed of room temperature and cooled samples. The resulting lifetimes were used to discover the influence of the different non-radiative decay processes and the influence of temperature and concentration on those processes. The main processes of non-radiative decay are energy migration and cross-relaxation. It was concluded that at low concentrations $\text{NaLaF}_4:\text{Pr}^{3+}$ is an efficient quantum cutter. At higher concentrations the influence of concentration quenching lowers the efficiency significantly. It was also concluded that the influence of temperature was insignificant for low concentration samples. For high concentration samples the influence was bigger but not enough to reach the wanted efficiencies. Overall it was concluded that $\text{NaLaF}_4:\text{Pr}^{3+}$ is a good quantum cutting material at concentrations of at most 10%.

1. Abstract
2. Contents
3. Introduction
4. Theory
 - a. Energy Levels of Pr^{3+}
 - b. Cascade Emission
 - c. Transitions
 - i. Radiative decay
 - ii. Energy migration
 - iii. Cross-relaxation
5. Experimental
 - a. Sample preparation
 - b. Measurements
 - i. Concentration dependence
 - ii. Temperature dependence
6. Results and Discussion
 - a. Concentration dependence
 - i. Emission spectra
 - ii. Lifetime measurements
 - b. Temperature dependence
 - i. Emission spectra
 - ii. Lifetime measurements
7. Conclusion

Introduction

Lanthanides are used in luminescent materials in several applications such as fluorescent tubes, lasers and televisions. In fluorescent lamps phosphors convert the ultraviolet radiation emitted by mercury gas into visible light. Mercury has the disadvantage that it is a liquid that must first evaporate before radiation can occur and this leads to a start-up time for such lamps. Without this start-up time fluorescent lamps could be implemented in for example copying machines and car brake lights. Therefore research into different Luminescent materials is necessary to find a better combination of a discharge gas providing the UV radiation to excite a phosphor and the phosphor itself. This is especially true in cases where the Hg gas is replaced by a gas that emits higher energy UV photons to use. For instance xenon gas could be a good replacement for Hg, but since Xe emits at 172nm the required energy to operate is a lot higher than with Hg gas that emits at 254nm. To make this replacement efficient phosphors with a quantum efficiency higher than unity will be needed.[1]

One way to achieve this efficiency is by the use of so called quantum cutters, these are materials that upon absorbing one high energy (UV) photon emit several photons of lower energy in the visible range of the spectrum. Several of those materials have already been found mostly consisting of a Lanthanide ion inside a crystal lattice such as Eu^{3+} doped LiGdF_4 or in our case Pr^{3+} in a fluoride crystal.

To achieve an as high as possible quantum efficiency research needs to be done on the influence of the crystal lattice on the luminescent ion, the concentration of the dopant and the temperature effects. The crystal lattice surrounding the phosphor influences the splitting of the energy levels of the ion and as such the wavelength at which optimal excitation can take place and the wavelengths of the emitted photons, allowing influence on the colour of light of the lamp. Concentration and temperature effects both have influence on the ratio of radiative and non-radiative decay of the excited state of the phosphor. Whereas higher temperature increases the possibility of phonon relaxation processes, a higher concentration will lead to concentration quenching and more cross-relaxation, where energy is transferred to a nearby luminescent ion that is then excited into a state from where non-radiative decay follows. A longer distance of energy transfer over the like luminescent ions increases the probability it finds a quencher such as a cross-relaxing pair or a defect. All these processes will ultimately lead to a lower quantum efficiency.

In this thesis the effects of the concentration and temperature on the emission and decay times of the $^1\text{S}_0$ and $^3\text{P}_0$ emission for Pr^{3+} in a NaLaF_4 lattice will be investigated. Discovering the scope of influence of the different processes on the emission lifetime of $\text{NaLaF}_4:\text{Pr}^{3+}$ will lead to better understanding and possibly the development of more efficient quantum cutting phosphors.

Theory

Energy Levels of Pr³⁺

The energy levels of Lanthanide ions such as Pr³⁺ result from different configurations of electrons in the 4f orbitals. Seven 4f orbitals allow for a total of 14 electrons. The two electrons in the 4f shell Pr³⁺ allow for 91 configurations creating a rich energy structure allowing for absorption and emission in a wide area of wavelengths. These energy levels have been studied in detail and have been categorized by Dieke resulting in the Dieke Diagram [2], displaying the 4fⁿ energy levels of the lanthanide ions in a LaCl₃ host lattice.

In figure 1 the free ion energy level diagram of Pr³⁺ is shown. There is a large gap between the ¹S₀ level around 47000cm⁻¹ (~215nm) and the next lower ³P₂ level. Two-step (cascade) emission from the ¹S₀ level is possible (see below) but only if the 4f5d state is at higher energy than the ¹S₀ level. The position of the lowest 4f5d level for Pr³⁺ in a variety of hosts has been investigated by Krumpel et al. [3] showing that for Pr³⁺ in NaLaF₄ the position is similar to that in YF₃, where the 4f5d state is situated above the ¹S₀ level.

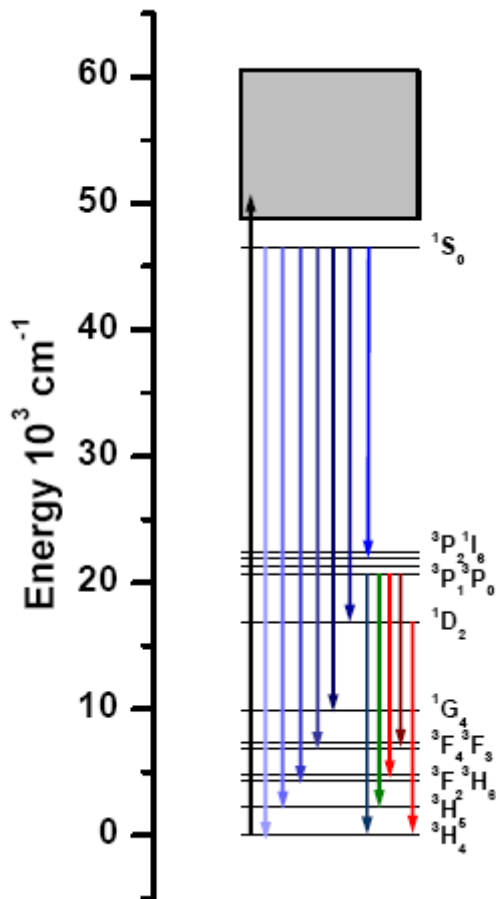


Fig 1. Energy Diagram of Pr³⁺. [4]

Cascade Emission

Cascade Emission is a type of quantum cutting where a luminescent material that upon being excited by 1 photon, most often in the Ultraviolet range, will emit two or more photons in usually the visible range of the spectrum. This happens when an excited ion radiatively decays to an intermediate energy level and, after possible relaxation, shows a radiative transition into a lower energy level. The high excited state falls down in multiple steps just like a cascade. This process can lead to quantum efficiencies beyond unity and is therefore a very interesting field for research. It is observed in several rare earth ions hosted in a rightly tailored crystal lattice and much research is done into applicable materials using this process. Other forms of quantum cutting make use of for instance cross-relaxation to excite two luminescent centers of a different element than the originally excited ion.[5]

In Pr^{3+} cascade emission [6] happens due to excitation into the 4f5d band followed by relaxation to the 1S_0 level which allows the radiative transition $^1S_0 \rightarrow ^1I_6$, followed by relaxation into the 3P_0 level that can then emit through the $^3P_0 \rightarrow ^3H_6, ^3H_4, ^3F_2$ transitions. This process yields upon excitation by 1 UV photon the emission of a blue (406nm) and a green (482nm) or red (608nm) photon. To achieve these emissions the ion is placed in a host lattice, in this research a NaLaF_4 crystal, that is chosen based on the placement of the 4f5d band of the Pr^{3+} due to the lattice influences. The ionic strength of NaLaF_4 combined with its weak crystal field place the lowest 4f5d level above the 1S_0 . [3]

The cascade process allowing for more efficient emission is hampered by several processes such as cross-relaxation and concentration quenching that will be explained in more detail later in this chapter.

Transitions

After excitation the excited state has multiple paths to relax back down to its ground state. For this transition multiple options are viable, in our case especially radiation and cross-relaxation. Although phonon relaxation is an option in a lot of kind systems this is not relevant for this research as the phonon energy is too low to be able to serve as a transition path since phonon relaxation becomes improbable if more than five phonons are needed to bridge the energy gap. Since the phonon energy of NaLaF_4 is circa 400cm^{-1} five phonons are not enough to bridge the gap between the 1S_0 and 3P_2 levels which is approximately 25000cm^{-1} . Even for the lower energy levels 3P_0 and 1D_2 the gap to the next level is several times larger than the energy of five combined phonons Therefore in this chapter we will only discuss the systems of radiative relaxation, energy migration and cross-relaxation.

Radiative Decay

Even though radiative decay of electrons from one $4f^n$ configuration to another $4f^n$ configuration is strictly forbidden due to the absence of a electric dipole change the relaxation can still occur because of slight mixing of the $4f^{n-1}5d^1$ orbital with the $4f^n$ state. Since transition to the $4f^{n-1}5d^1$ state leads to a dipole change the radiative decay is no longer strictly forbidden. The probability of a radiative transition is strongly dependent on how much of the $4f^{n-1}5d^1$ is mixed in with the $4f^n$ level. The amount of $4f^{n-1}5d^1$ mixed in determines the dipole change and as such the probability of transition. This probability is also influenced strongly by the host lattice and the luminescent ion.

Energy migration

The main alternative to radiative decay in $\text{NaLaF}_4:\text{Pr}^{3+}$ is partial energy transfer. The process where the relaxation of one ion is combined with the simultaneous excitation of another, this can happen between either different or like ions. This allows the energy to hop from a Pr^{3+} ion to a nearby previously unexcited Pr^{3+} ion, leading to energy migration. The rate of energy transfer is mainly influenced by the distance between the ions. The higher the concentration of Pr^{3+} in the crystal the higher the mean distance traveled by the excitation energy, this leads to an increased probability that the energy ends up in a so called 'trap', most often a defect in the crystal or a cross-relaxing pair of Pr^{3+} ions as later explained, wherefrom no radiation can occur, as such the excitation energy is lost. This phenomenon is called concentration quenching and will account for decreased quantum efficiencies in higher concentrated samples. Energy migration can happen from all energy levels of Pr^{3+} .

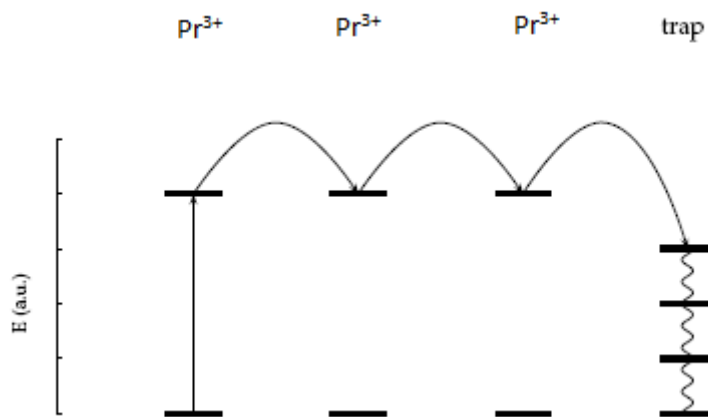


Fig 2. Energy migration and subsequent concentration quenching by energy migration in Pr^{3+} . [7]

Cross-relaxation

The way cross-relaxation can affect the quantum efficiency of the phosphor is if the energy released by the relaxation in one ion can excite a nearby ion from its ground state to a level from which thermal relaxation occurs. For cross-relaxation to occur the 2 ions need to have a transition that is comparable in energy and need to be close together, there is a need for a resonance condition for cross-relaxation to occur. For instance in Pr^{3+} the energy difference between the $^1\text{D}_2$ and the $^1\text{G}_4$ levels is comparable to the difference between the appropriate Stark components of the $^3\text{H}_4$ and $^3\text{F}_4$ levels. This leads to a case where the relaxation from $^1\text{D}_2$ to $^1\text{G}_4$ level is coupled with the excitation of another ion from the $^3\text{H}_4$ to the $^3\text{F}_4$ level from which no radiation occurs. The $^1\text{S}_0 \rightarrow ^3\text{P}_0$ transition and all other transition from the $^1\text{S}_0$ have no resonance conditions and cross-relaxation will not occur from this level, it only happens from the $^1\text{D}_2$ and the $^3\text{P}_0$ levels. Further research of the influence of concentration quenching and cross-relaxation of Pr^{3+} has been reported by Naik, Karanjikar and Razvi [8]

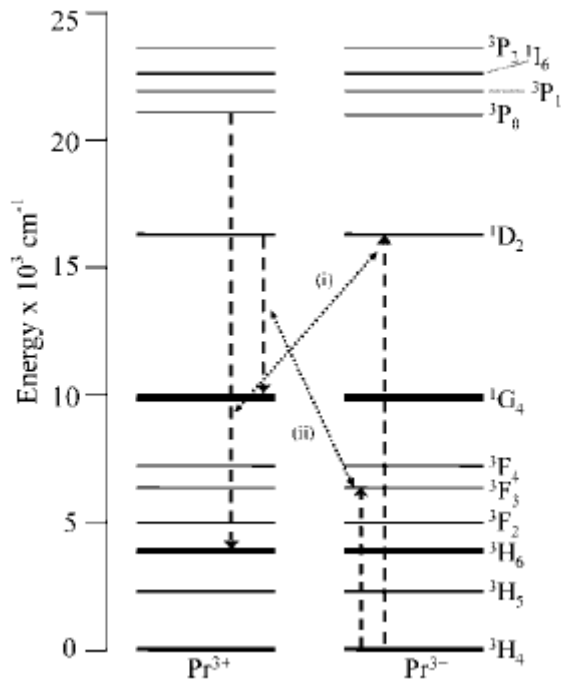


Fig 3. Cross-relaxation of Pr^{3+} (i) cross-relaxation mechanism of populating the 1D_2 level, (ii) Cross-relaxation of the $[^1D_2, ^3H_4] \rightarrow [^1G_4, ^3F_{3,4}]$ pair quenching the $^1D_2 \rightarrow ^3H_4$ emission. [9]

Experimental

Sample Preparation

All samples were prepared by the Department of Chemical Engineering of the University of Applied Sciences Münster. Sample preparation was performed by the so called "Mix and Fire" method. As starting materials high purity NaF, LaF_3 , and PrF_3 were used. Appropriate blends were sintered for 6 h at 700 °C in a Nitrogen stream. [3]

Measurements

Optical spectroscopy measurements were taken. Measurements were taken using a nitrogen-cooled CCD and a spectrapro -300i 0.300m triple grating monochromator. Decay measurements were taken using an oscilloscope. Excitation was done by an ArF excimer laser pulsing at 193nm

For the low temperature measurements a cryostat was used with liquid Helium cooling.

Results and Discussion

Concentration dependence

First we will discuss the measurements of Pr^{3+} at different concentrations to determine which relaxation path becomes dominant when the concentration increases. Therefore two peaks were interesting, first the peak at 406nm representing the $^1\text{S}_0 \rightarrow ^1\text{I}_6$ transition and secondly the peak at 608nm representing the $^3\text{P}_0 \rightarrow ^3\text{H}_6$ transition. This because the $^1\text{S}_0 \rightarrow ^1\text{I}_6$ is a transition from the relatively isolated $^1\text{S}_0$, an interesting starting level for quantum cutting because there is no possible cross-relaxation and is thus only quenched by energy migration (concentration quenching). The $^3\text{P}_0$ transitions are required for efficient quantum cutting but could suffer greatly from quenching by cross-relaxation.

Emission spectra

Emission spectra at room temperature were taken for the 406 and the 608nm peaks and shown in figure 4 and 5.

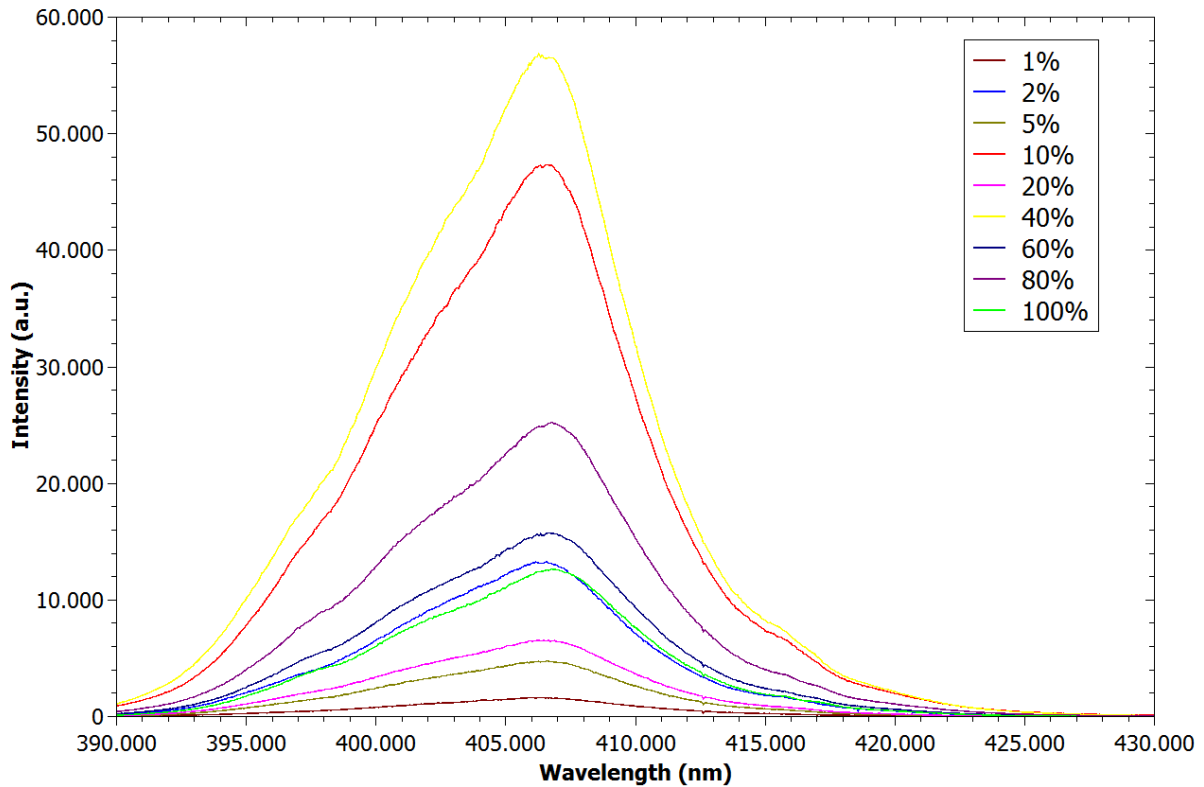


Fig 4. Emission spectrum of the 406nm peak of different concentrated samples of $\text{NaLaF}_4:\text{Pr}^{3+}$.

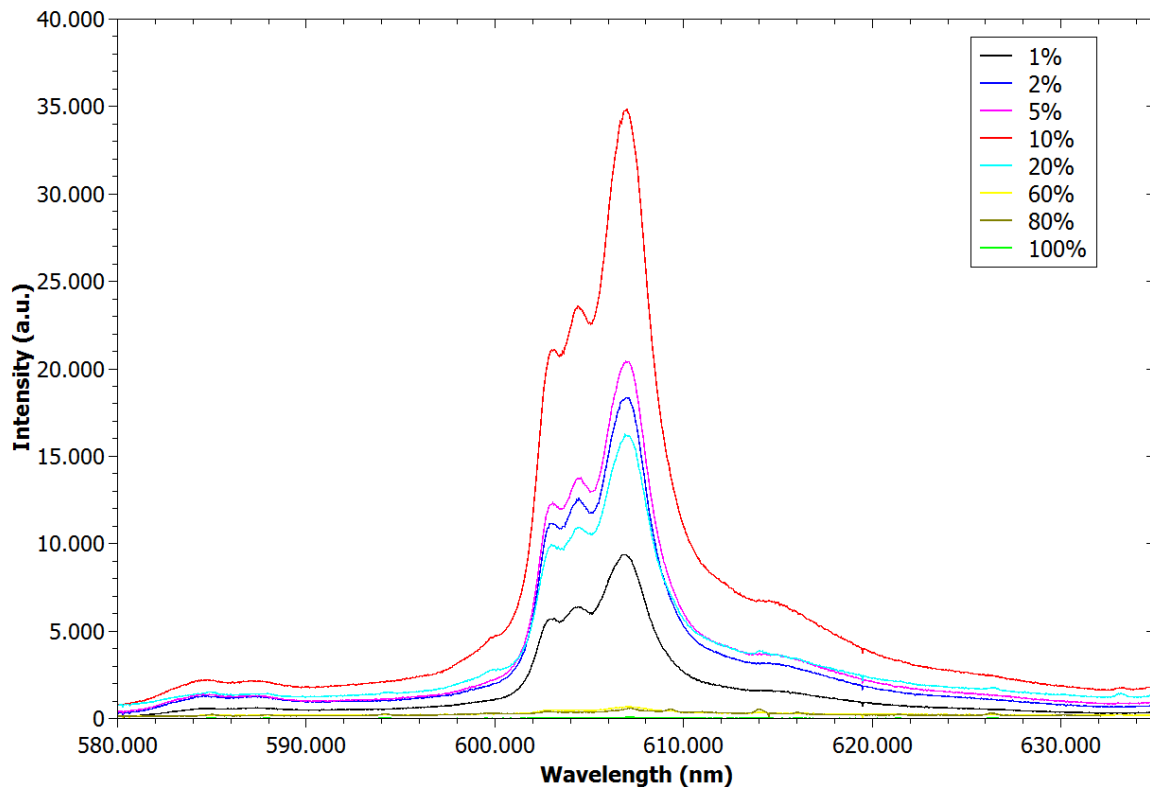


Fig 5. Emission spectrum of the 608nm peak of different concentrated samples of $\text{NaLaF}_4:\text{Pr}^{3+}$.

It can be seen that especially the 608nm emission is quenched significantly at higher concentrations.

Lifetime measurements

To gain insight in the processes governing the quantum cutting efficiency luminescence decay curves were recorded for two transitions, the $^1\text{S}_0 \rightarrow ^1\text{I}_6$ transition with its emission at 406nm and the $^3\text{P}_0 \rightarrow ^3\text{H}_6$ with its emission at 608nm.

First for the $^1\text{S}_0 \rightarrow ^1\text{I}_6$ transition decay curves are shown in figure 6 which are fitted with an single exponential fit to calculate the lifetime, those are shown in figure 7 To obtain those measurements the samples were excited by an ArF excimer laser at 193nm and measurements were recorded at 406nm.

In figure 4 it can be seen that the steepness of the decay curve increases as the concentration gets higher corresponding with a decline in lifetimes in figure 5. This decline is caused by energy migration leading to concentration quenching. At higher concentrations the mean path of energy migration gets longer and as such the probability of encountering a trap increases, this leads to shorter lifetimes. The relatively small declines in lifetimes also indicate that no cross-relaxation is happening as was expected; cross-relaxation would have caused a much steeper decline in lifetimes.

It can be concluded that the concentration influence on the $^1\text{S}_0 \rightarrow ^1\text{I}_6$ emission is as expected governed by concentration quenching and cross-relaxation plays no effect. The lifetime drops only $0,336\mu\text{s}$ from $0,598\mu\text{s}$ at 1% to $0,262\mu\text{s}$ at 100% with the lifetime only dropping below $0,4\mu\text{s}$ at concentrations above 40%. This indicates that the $^1\text{S}_0$ level is an excellent starting level for quantum cutting even at high concentrations.

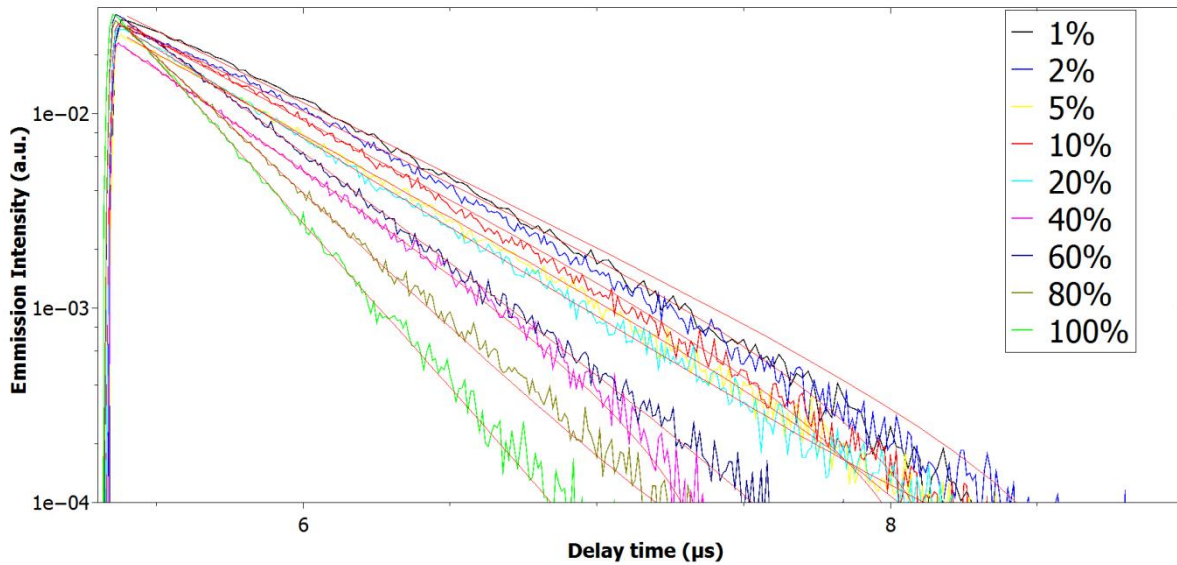


Fig 6. Decay curves of the 406nm emission at room temperature for different concentrated samples of $\text{NaLaF}_4:\text{Pr}^{3+}$ excited at 193nm with their respective single exponential fit.

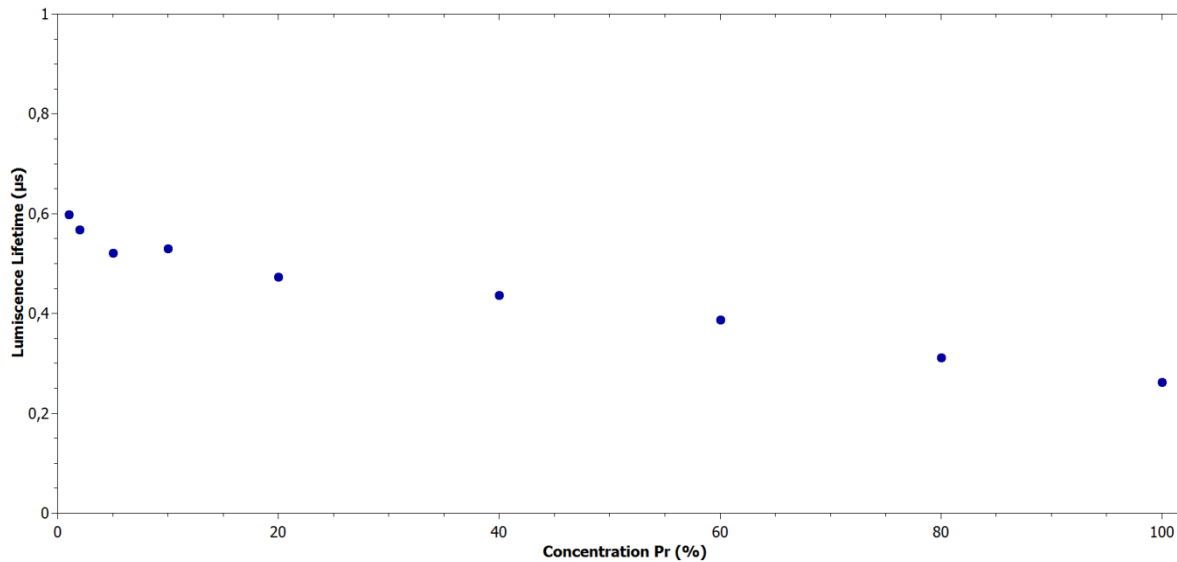


Fig 7. Calculated (by single exponential fit) lifetimes of the 406nm emission at room temperature for different concentrated samples of $\text{NaLaF}_4:\text{Pr}^{3+}$.

Secondly the decay curves for the ${}^3\text{P}_0 \rightarrow {}^3\text{H}_6$ emission that were measured at 608nm are shown in fig 8 and the calculated lifetimes using a single exponential fit of the peaks at 482nm, 608nm, 640nm in fig 9. Only the decay curves of the 608nm emission are shown because of the similarities between the three emissions. Measurements at higher concentrations were cut short to increase resolution in order to gain a better fit.

At concentrations of 40% and above a second peak in intensity can be seen just after 8μs most likely caused by an instrumental artifact. The decay curves decline a lot faster in the higher concentrations than in the 406nm emission measurements in figure 6. In the lower concentrated samples (10% or less) a small rise in intensity can be seen after the pulse. This could indicate a small delay before the ${}^3\text{P}_0$ level is saturated or a repopulated ${}^3\text{P}_0$ level by cross-relaxation, since this process is still fairly slow at these concentrations. In figure 9 the lifetimes are shown showing a steep decline in lifetimes till a concentrations of 40% where the decline flattens out. The decline at 40% and above is similar to that

in the 406nm emission measurement in figure 5. From 1% to 20% the lifetime drops from 17,3 μ s to 0,948 μ s ending at 0.194 μ s at 100% indicating that cross-relaxation plays a big role in these emissions. It should be noted that although there are small differences between the lifetimes of the different emission wavelength at low concentrations these are quickly evened out when the concentration rises.

It can be concluded that the emission from the 3P_0 and its surrounding levels have fairly long lifetimes when compared to the 1S_0 emission but decline very rapidly. At 40% the lifetimes of the 1S_0 emission is higher than those of the second step in the cascade. The second step is hampered a lot by cross-relaxation causing higher concentrations of Pr^{3+} to be a lot less efficient. The cross-relaxation has such a big influence that the influence of concentration quenching becomes almost irrelevant.

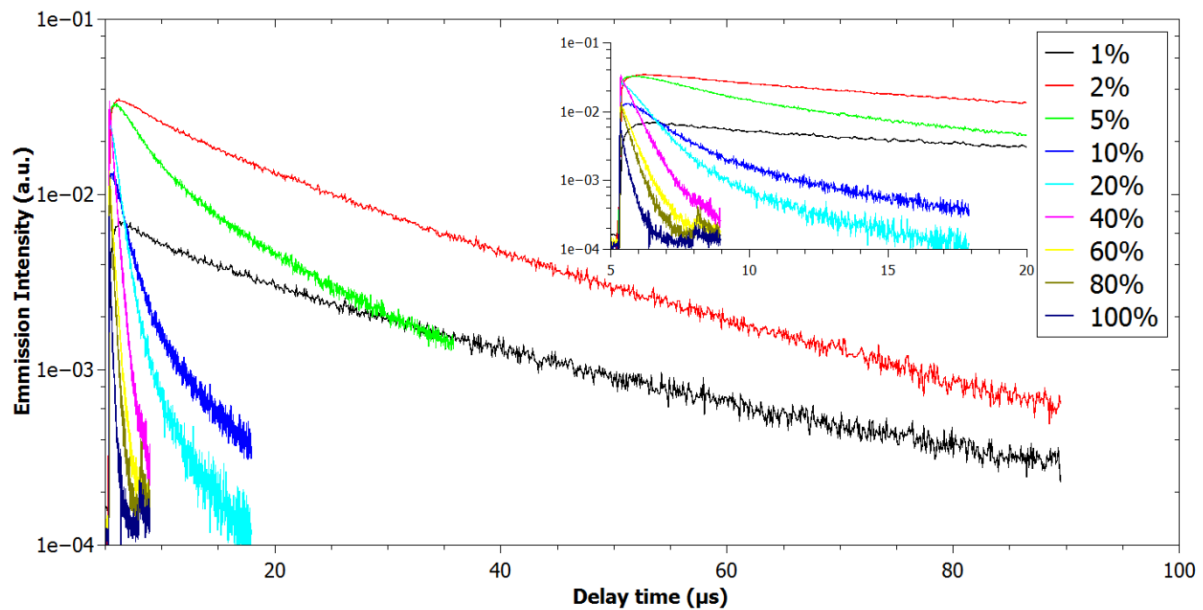


Fig 8. Decay curves of the 608nm emission at room temperature for different concentrated samples of $NaLaF_4:Pr^{3+}$ excited at 193nm.

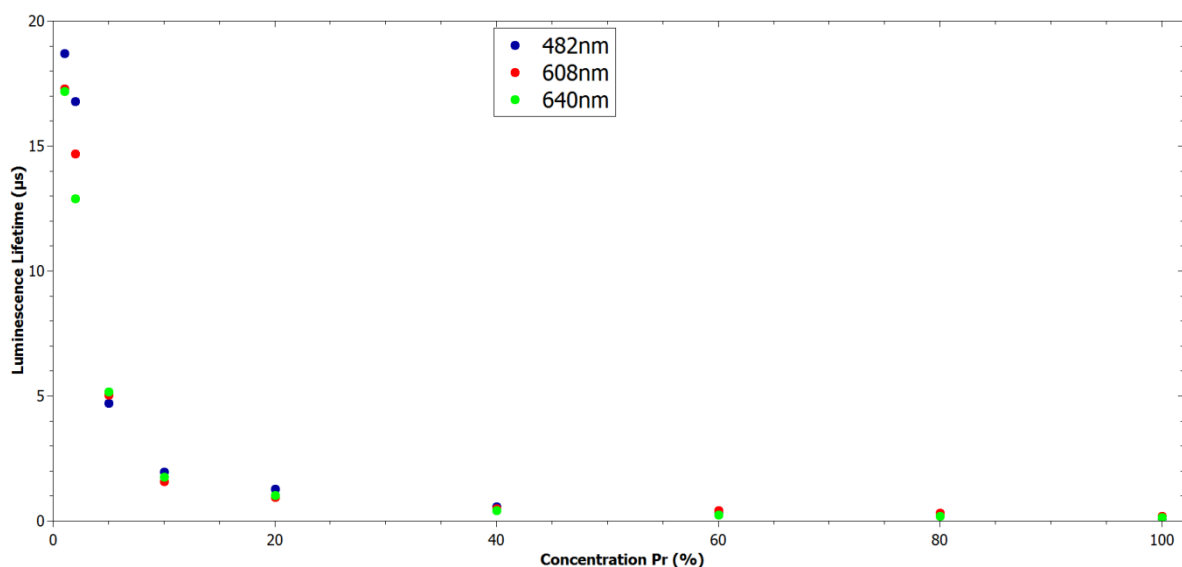


Fig 9. Calculated (by single exponential fit) lifetimes of the 482nm, 608nm and 640 nm emissions at room temperature for different concentrated samples of $NaLaF_4:Pr^{3+}$.

Temperature Dependence

Measurements were taken of the 1% and 100% Pr^{3+} samples were taken at different temperatures to observe the influence of temperature on the various relaxation paths. Once again the 406nm and 608nm emissions, coming from the $^1\text{S}_0 \rightarrow ^1\text{I}_6$ and the $^3\text{P}_0 \rightarrow ^3\text{H}_6$ transitions, were investigated to gain insight in the temperature dependence.

Emission spectra

Emission spectra were recorded of the 406nm and the 608nm peaks at varying temperatures for the 1% and the 100% $\text{NaLaF}_4:\text{Pr}^{3+}$ samples and are displayed in figures 10 through to 13.

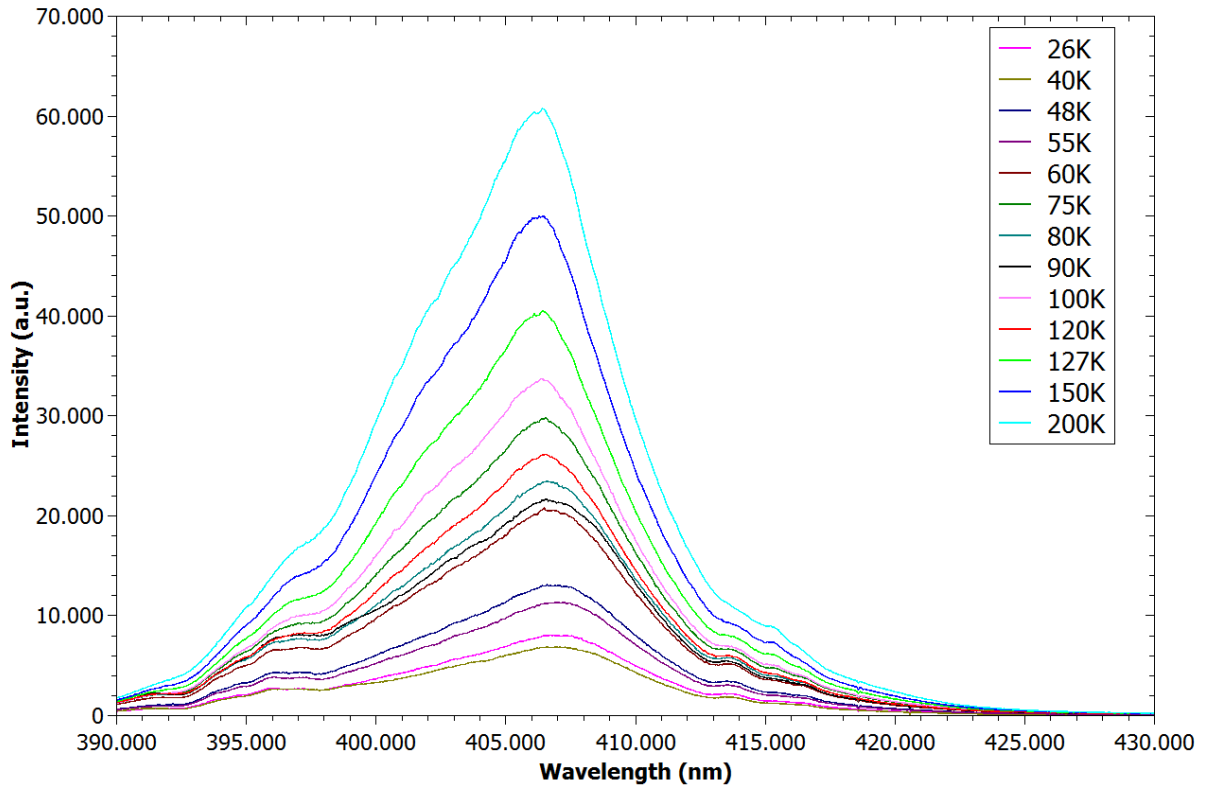


Fig 10. Emission spectrum for the 406nm peak of the 1% $\text{NaLaF}_4:\text{Pr}^{3+}$ sample at varying temperatures.

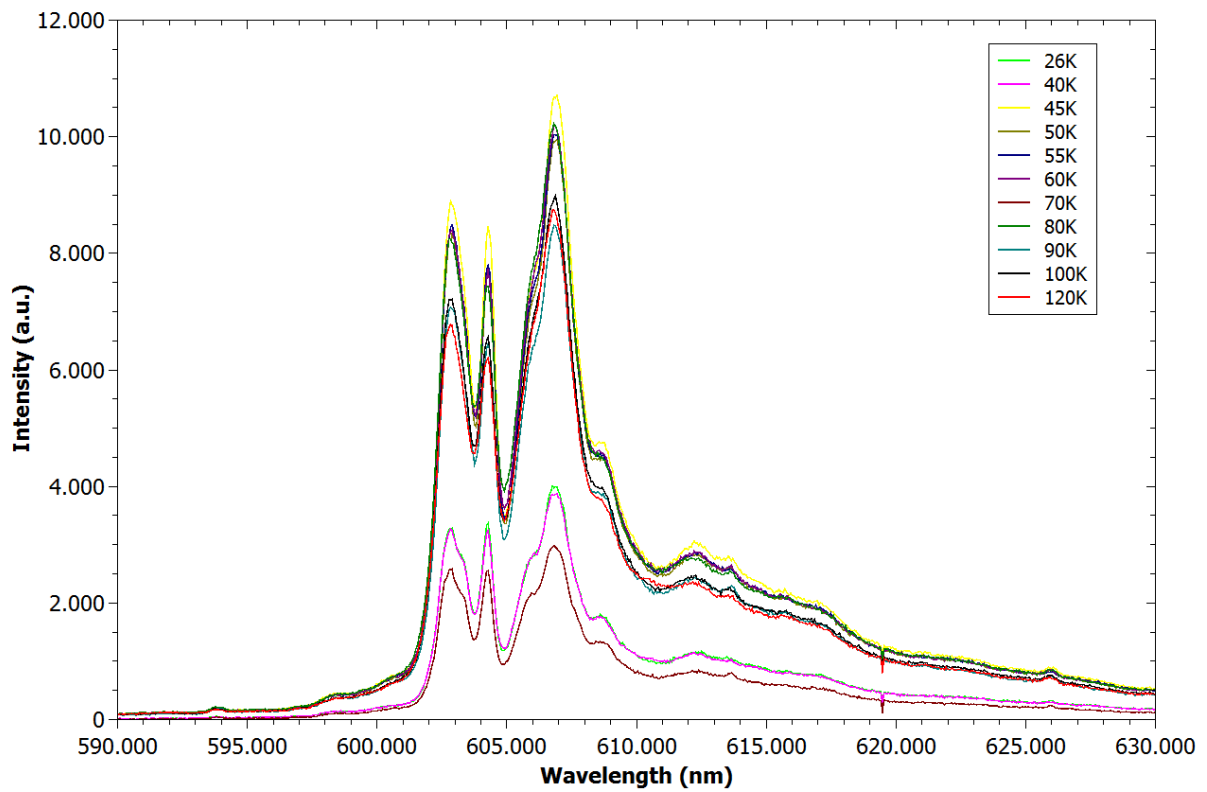


Fig 11. Emission spectrum for the 608nm peak of the 1% NaLaF₄:Pr³⁺ sample at varying temperatures.

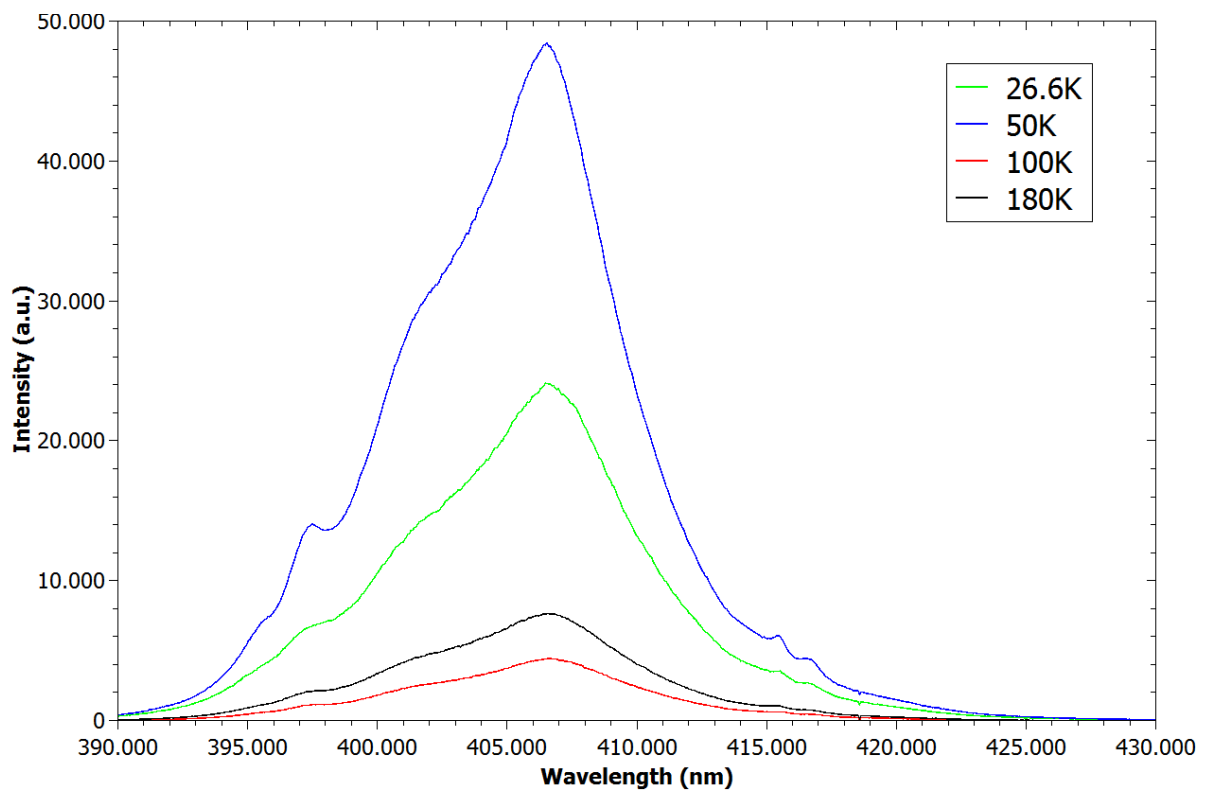


Fig 12. Emission spectrum for the 406nm peak of the 100% NaLaF₄:Pr³⁺ sample at varying temperatures.

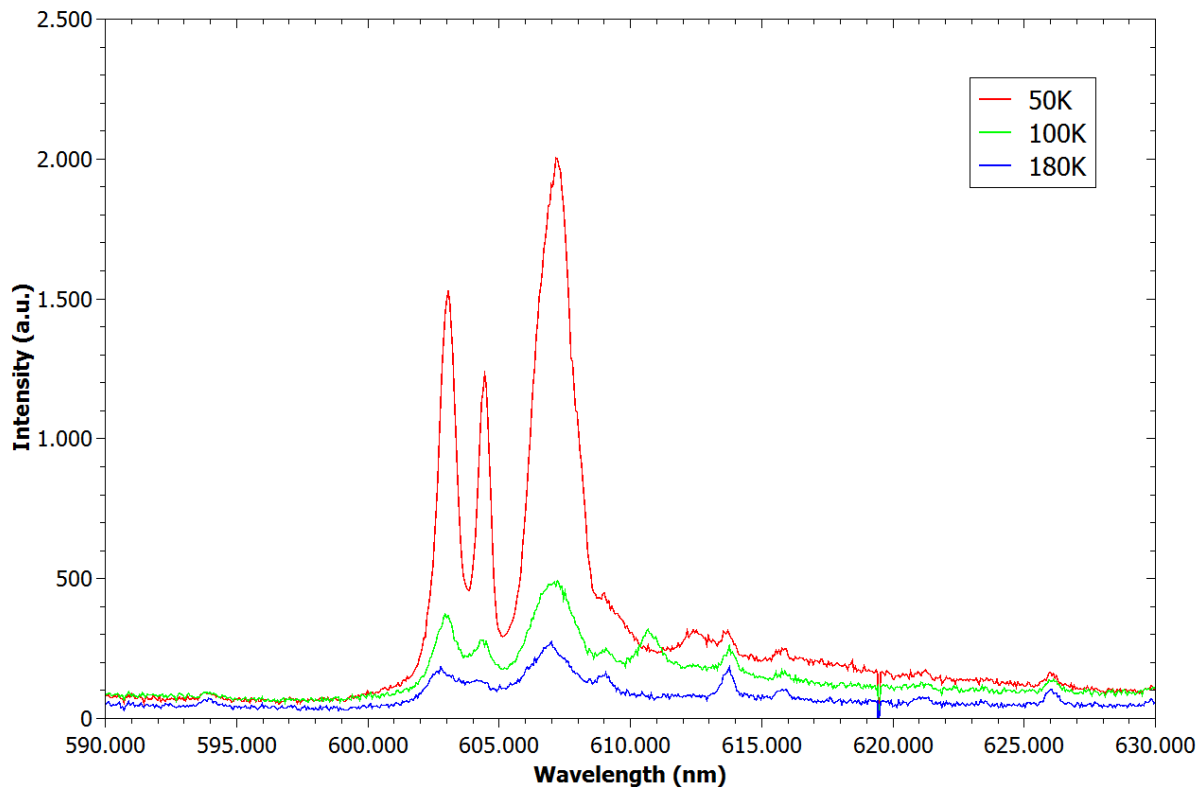


Fig 13. Emission spectrum for the 608nm peak of the 100% NaLaF₄:Pr³⁺ sample at varying temperatures.

Lifetime measurements

In figure 14 the decay curves of the 406nm emission of the 1% NaLaF₄:Pr³⁺ are portrayed at various temperatures; the room temperature decay curve is taken from the concentration dependence measurements. All decay curves were fitted with a single exponential fit to determine the lifetime. Those lifetimes are displayed in figure 15.

The decay curves of the 1% 406nm emission are all relatively sloped the same and several of them overlap. Just after excitation there seems to be a slight delay before the curve starts to decay especially at the lower temperatures. This might indicate a degree of saturation of the sample.

Looking at the lifetimes it can be seen that the lifetime stays fairly constant over the increase in temperature, almost perfectly in line including the room temperature lifetime. At all temperatures the lifetime is about 0,55μs.

As expected the lifetime of the ¹S₀ transition of the 1% Pr³⁺ sample seems to be temperature independent. This is as to be expected since at this low concentration energy migration is negligible to begin with so the effect on temperature on this process will not result in a big change of lifetime. Furthermore the ¹S₀ transition displayed no cross-relaxation even at much bigger concentrations, so the temperature on this process is not relevant here. Therefore the lifetime is purely determined by the radiative rate which is not dependant on the temperature.

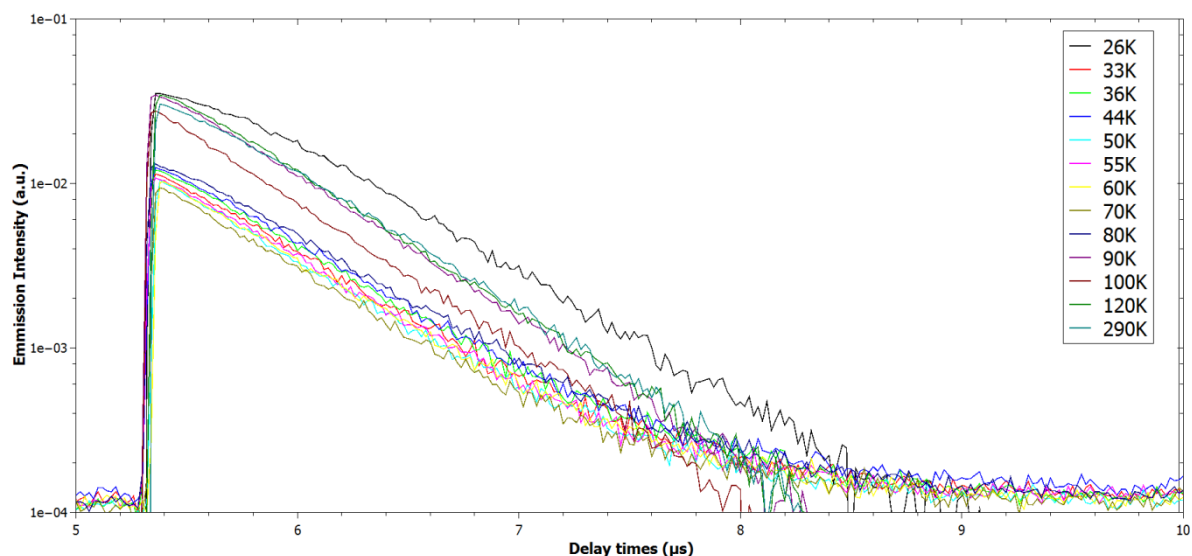


Fig 14. Decay curves of the 406nm emission from the 1% NaLaF₄:Pr³⁺ sample at various temperatures excited at 193nm.

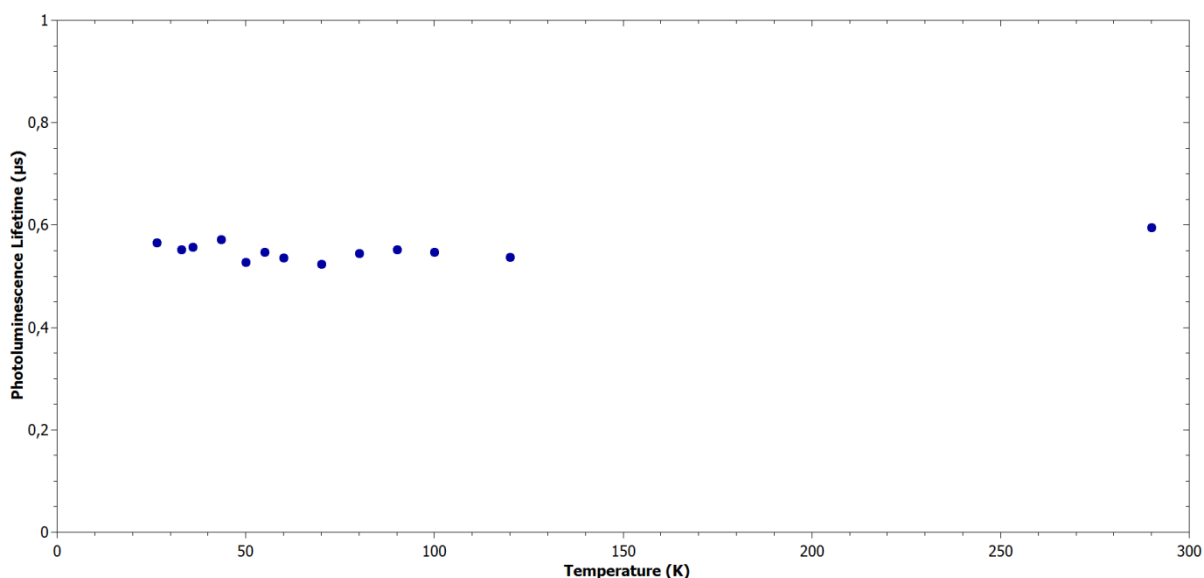


Fig 15. Calculated (by single exponential fit) lifetimes of the 406nm emission of the 1% NaLaF₄:Pr³⁺ sample at various temperatures.

In figure 16 the decay curves of the 608nm emission of the $^3P_0 \rightarrow ^3H_6$ transition are displayed measured at various temperatures, once again the room temperature decay curve is taken from the concentration dependence measurements. The decay curves were fitted using a single exponential fit to determine the lifetime of the emission, the calculated lifetimes are displayed in figure 17.

In figure 16 it can be seen that the differences between the decay curves at various temperatures are minimal with almost all curves seeming to overlap. Also the small rise after excitation that was seen in the room temperature measurements is seen at lower temperatures as well although it can be less clear. This could be possibly explained by the fact that cross-relaxation will be slower at low temperatures meaning repopulation of the 3P_0 level would be less frequent. A difference with the decay curves of the cooled samples and the room temperature decay curve is observed indicating that temperature does play a part in the lifetime of the $^3P_0 \rightarrow ^3H_6$ transition of NaLaF₄:Pr³⁺.

The lifetimes calculated using a single exponential fit are shown in figure 17. There it can be seen that although there are small variations between the different temperatures the lifetimes seem to be fairly constant at approximately 25 μ s. The increase of the lifetimes from the 26 and 35K measurements and the 40K and above is probably an error in measurement or an instrumental artifact since it can not be properly explained. From the 40K sample the lifetimes seem to decline very slowly with increasing temperature from the approximately 25 μ s at lower temperatures till 17 μ s at room temperature. This could be explained by the fact that even though the concentration is very low some cross-relaxation will still occur from the 3P_0 level as explained earlier, at lower temperatures this process will be less frequent leading to longer lifetimes.

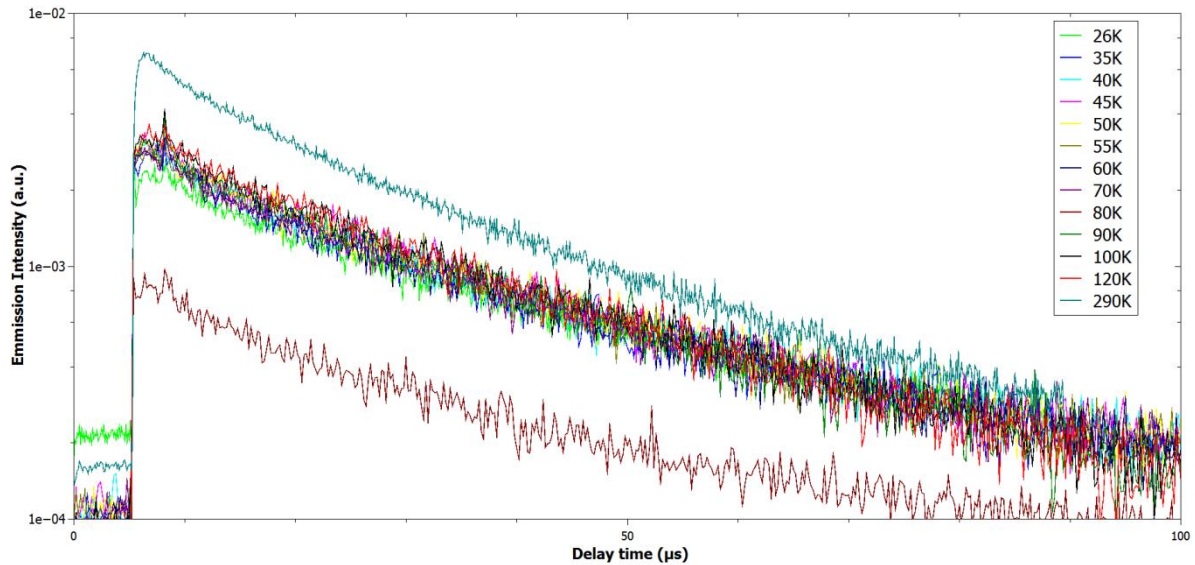


Fig 16. Decay curves of the 608nm emission from the 1% NaLaF₄:Pr³⁺ sample at various temperatures.

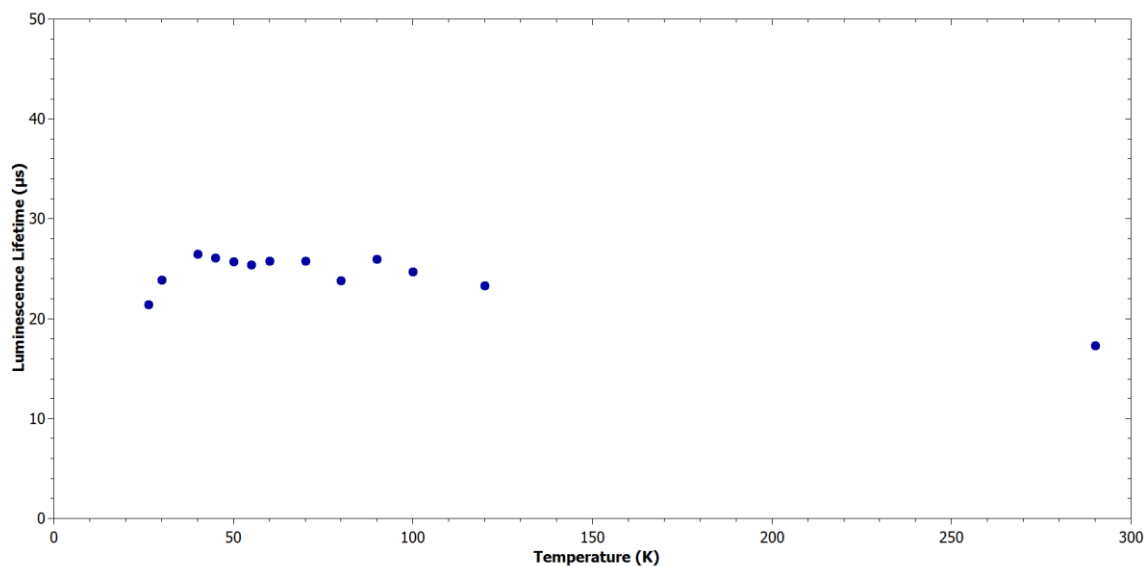


Fig 17. Calculated lifetimes of the 608nm emission of the 1% NaLaF₄:Pr³⁺ sample at various temperatures.

In conclusion of the temperature dependence measurements of the 1% NaLaF₄:Pr³⁺ sample it can be said that lowering the temperature doesn't increase the lifetime of the emission at either 406nm or 608nm. Thus lowering the temperature will not increase the quantum efficiency of this phosphor substantially.

This is as expected for samples of such low concentration since the processes that are influenced by temperature such as cross-relaxation and energy migration can barely occur at this concentration.

To gain insight in the temperature dependent processes measurements were taken of the 100% NaLaF₄:Pr³⁺ sample at 406nm and 608 nm. At this concentration cross-relaxation and energy migration was shown to be of big influence in the concentration dependent measurements. Since these processes are strongly influenced by temperature a comparison between the ¹S₀→¹I₆ and ³P₀→³H₆ transition was made.

In figure 18 the decay curves of the ¹S₀→¹I₆ transition at 406nm are displayed for various temperatures. Some slight saturation can once again be observed just after excitation and the instrumental artefact of a second peak in intensity displayed earlier can once again be seen at higher temperatures. Furthermore it seems that the slopes of the curves are fairly identical across the various temperatures.

The curves were fitted with a single exponential fit to calculate the lifetimes and shown in figure 20.

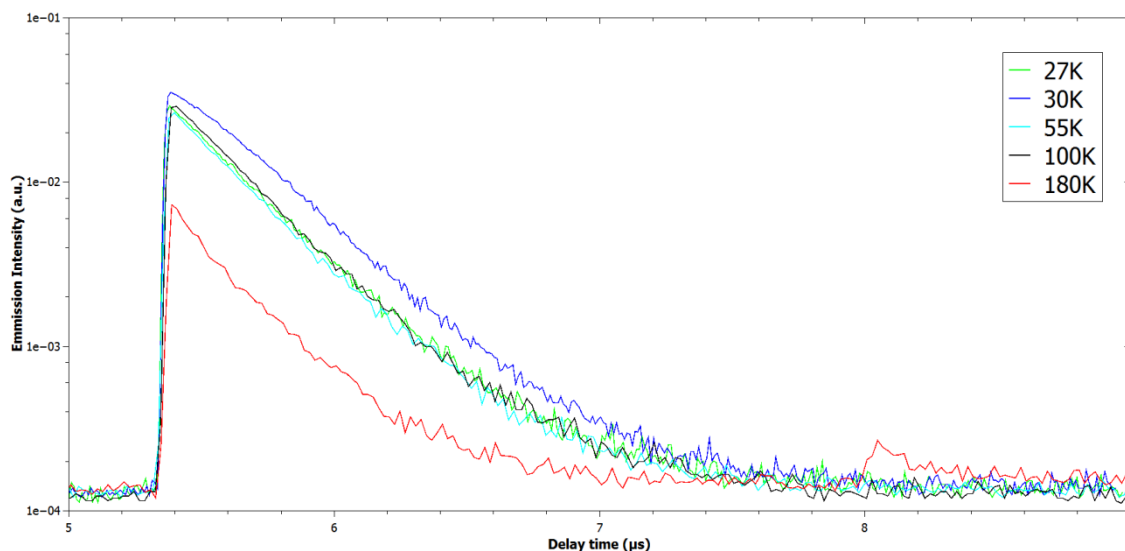


Fig 18. Decay curves of the 406nm emission from the 100% NaLaF₄:Pr³⁺ sample at various temperatures.

In figure 19 the decay curves of the ³P₀→³H₆ transition at 608nm are displayed at varying temperatures. Some saturation and the instrumental artefact at higher temperatures can be observed here also. But the slopes of the curves vary substantially with varying temperature for the 608nm emission. This indicates that temperature has a significant effect on the efficiency of the ³P₀→³H₆ transition.

Lifetimes were determined using a single exponential fit to the decay curves and displayed in figure 20 alongside the calculated lifetimes of the ¹S₀→¹I₆ transition to emphasize the differences. For the 406nm emission it can be concluded that even at a concentration of 100% Pr³⁺ the luminescence is temperature independent staying constant at 0,26μs. The 608nm is heavily influenced by temperature at very low temperatures with a lifetime of 1,19μs at 27K dropping to 0,28μs at 55K, a decline by a factor of 6. Increasing the temperature above 55K does not significantly impact the lifetime, staying fairly constant even up to room temperature where the lifetime is 0,19μs. Since the trend is visible at such low temperatures the room temperature decay curves and lifetimes were not included here.

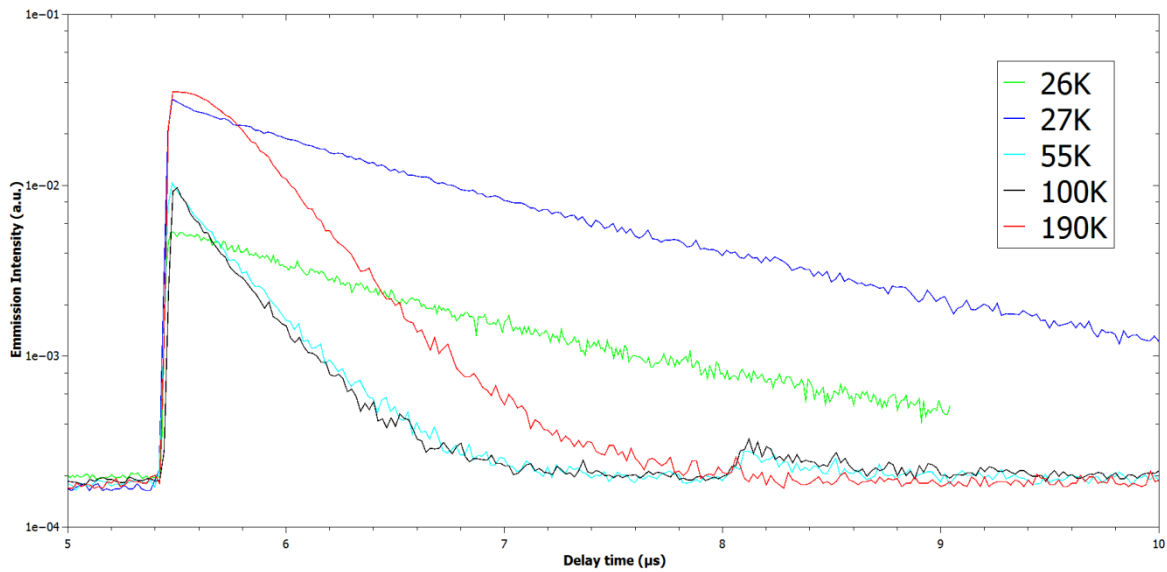


Fig 19. Decay curves of the 608nm emission from the 100% NaLaF₄:Pr³⁺ sample at various temperatures.

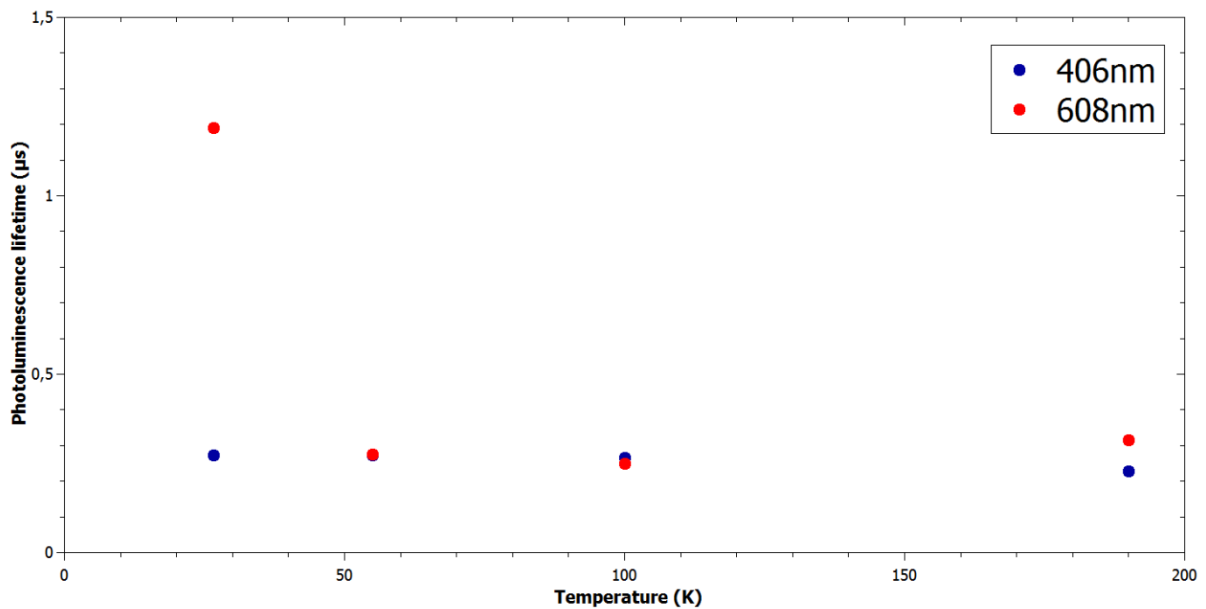


Fig 20. Calculated lifetimes of the 406 and 608nm emissions of the 100% NaLaF₄:Pr³⁺ sample at various temperatures.

As expected it can be concluded that the $^1S_0 \rightarrow ^1I_6$ transition displays no cross-relaxation and negligible energy migration since both those processes are heavily influenced by temperature and no difference can be seen at lower temperatures. A different case was seen for the $^3P_0 \rightarrow ^3H_6$ transition, also as expected, at very low temperatures the cross-relaxation and energy migration observed in the concentration studies is hampered severely causing an increase of the lifetime by a factor of 6. But this was only observed at temperatures around 30K and lifetimes stayed constant until the phosphor was cooled to temperatures below 55K.

Conclusion

Emission spectra and decay curves were successfully measured for all differently concentrated samples of $\text{NaLaF}_4:\text{Pr}^{3+}$. The decay curves were fitted using a single exponential fit to calculate the luminescence lifetime of all samples. From those measurements it can be concluded that Pr^{3+} has two very different kinds of transitions. A distinct difference is observed between the $^1\text{S}_0 \rightarrow ^1\text{I}_6$ transition and the different transitions from the various ^3P levels. Where the $^1\text{S}_0 \rightarrow ^1\text{I}_6$ transition lifetime is almost concentration independent and as such is a good starting level for quantum cutting the second step of the cascade from the ^3P levels is severely hampered by cross-relaxation and concentration quenching leading to a fast diminishing efficiency at higher concentrations. At concentrations of 10% or higher the lifetimes of the emission is almost $1/10^{\text{th}}$ of the lifetime at 1%, decreasing to $1/100^{\text{th}}$ at 100%. Even though the decline is fast the samples with a concentration of 10% or less still have lifetimes long enough to allow efficient quantum cutting.

To study the influence of cross-relaxation and energy migration emission spectra and decay curves were also measured for the 1% and 100% concentrated $\text{NaLaF}_4:\text{Pr}^{3+}$ samples at lowered temperatures. The same divide between the $^1\text{S}_0 \rightarrow ^1\text{I}_6$ transition and those from the ^3P levels can be seen, as represented by the 608nm emission of the $^3\text{P}_0 \rightarrow ^3\text{H}_6$ transition. Whereas the $^1\text{S}_0 \rightarrow ^1\text{I}_6$ transition emission at 406nm was temperature independent for both the 1% and 100% concentrated samples the $^3\text{P}_0 \rightarrow ^3\text{H}_6$ transition showed a heavy influence of the temperature at 100% Pr^{3+} . Also it was seen that at a concentration of 1% almost no cross-relaxation and energy migration occurs, indicated by the fact that the 608nm emission lifetime was constant across all temperatures. If cross-relaxation or energy migration had occurred at this concentration lifetimes would have increased with lower temperatures because cross-relaxation and energy migration processes are slowed. At 100% $\text{NaLaF}_4:\text{Pr}^{3+}$ the influence of temperature was heavy for the 608nm with a steep increase of the lifetimes at temperatures below 55K. The lifetimes at 30K were 6 times higher than those at 55K or higher. It can be concluded that only at very low temperatures the cross-relaxation and energy migration is slowed enough to effectively increase the efficiency.

As expected all samples exhibited quantum cutting but the lifetime of the second step of the cascade dropped fairly quickly with increasing concentration, it was also shown that cooling the samples only increased the lifetime at very low temperatures.

It can be concluded that $\text{NaLaF}_4:\text{Pr}^{3+}$ is a suitable material for 2-photon luminescence especially at concentrations of 10% and lower. The first step emitting at 406nm is a good start because it is almost concentration and temperature independent. For the second step, especially at higher concentrations, cross-relaxation and concentration quenching play such a big part that a high efficiency is hard to attain. It was shown that cooling the samples to increase the efficiency required such low temperatures that practical implications are difficult at best.

Literature

- [1] René T. Wegh, Harry Donker, Koenraad D. Oskam, Andries Meijerink. Visible Quantum Cutting in $\text{LiGdF}_4:\text{Eu}^{3+}$ Through Downconversion, *Science* 283, 663-666 (1999)
- [2] Dieke, G. H. *Spectra and Energy Levels of Rare Earth Ions in Crystals* (Interscience Publishers, New York, 1968), 1st edition.
- [3] A. H. Krumpel, E. van der Kolk, D. Zeelenberg, A. J. J. Bos, K. W. Krämer et al. Lanthanide 4f-level location in lanthanide doped and cerium-lanthanide codoped NaLaF_4 by photo- and thermoluminescence. *J. Appl. Phys.* 104, 073505 (2008); doi: 10.1063/1.2955776
- [4] Benjamin Herden, Andries Meijerink, Freddy T. Rabouw, Markus Haase, Thomas Jüstel. Two-Photon Emission in $\text{NaLaF}_4:\text{Pr}$ and NaPrF_4 Revisited. *Poster REEC 2013*
- [5] Jiayue Sun, Yining Sun, Chun Cao, Zhiguo Xia, Haiyan Du. Near-infrared luminescence and quantum cutting mechanism in $\text{CaWO}_4:\text{Nd}^{3+}, \text{Yb}^{3+}$. *Applied Physics B* May 2013, Volume 111, Issue 3, pp 367-371
- [6] J.L. Sommerdijk, A. Bril, A.W. de Jager. Two photon luminescence with ultraviolet excitation of trivalent praseodymium. *Journal of Luminescence* 8, 341-343 (1974)
- [7] M. de Jong. Downconversion in CsCdBr_3 doped with Nd^{3+} and Yb^{3+} . *Bachelor's thesis*. 2009
- [8] R.C. Naik, N.P. Karanjikar and M.A.N. Razvi, Concentration quenching of fluorescence from $^1\text{D}_2$ state of Pr^{3+} in YPO_4 . *Journal of Luminescence* 54 139-144 (1992)
- [9] R. Naccache, F. Vetrone, A. Speghini, M. Bettinelli, and J. A. Capobianco. Cross-Relaxation and Upconversion Processes in Pr^{3+} Singly Doped and $\text{Pr}^{3+}/\text{Yb}^{3+}$ Codoped Nanocrystalline $\text{Gd}_3\text{Ga}_5\text{O}_{12}$: The Sensitizer/Activator Relationship, *J. Phys. Chem. C*, 112, 7750–7756 (2008)